A theoretical study of rotational and translational diffusion dynamics of molecules with a six-fold point symmetry adsorbed on a hexagonal lattice by neutron scattering

I. Calvo-Almazán[1,2], S. Miret-Artés[3] and P. Fouquet[1]

[1] Institut Laue Langevin, BP 156, F-38042 Grenoble Cedex 9, France
[2] Universidad de Zaragoza, Ciudad Universitaria, 50009 Zaragoza, Spain
[3] Instituto de Física Fundamental, Consejo Superior de Investigaciones Científicas, Serrano 123, 28006, Madrid, Spain

E-mail: calvoalmazan@ill.fr,fouquet@ill.eu

Abstract. A complete analytical model for the rotational and translational diffusion of molecules with a six-fold point symmetry on a hexagonal lattice is presented. It can be applied, in particular, to the diffusion of benzene molecules adsorbed flat on the basal plane of graphite in the case of incoherent scattering. Under the *weak hindered approximation*, the classical mechanics framework and making use of the Van Hove formalism of correlation functions, the intermediate scattering function and its Fourier transform, the scattering law are both obtained. They can then be expressed as sums of exponential decays or Lorentzian functions, respectively, containing the contribution of each of the dynamical processes taking place. In the case of benzene lying flat on the substrate we expect namely: translational diffusion, continuous rotations of isolated molecules and hindered rotations of molecules within clusters. Each particular diffusive mechanism can be recognized owing to its particular signature in the dependence of the quasi-elastic broadening on the momentum transfer.

PACS numbers: 62.25.-g, 68.35.Af, 68.43.Jk, 68.49.-h, 81.05.U-

Submitted to: *J. Phys.: Condens. Matter*

1. Introduction

The study of diffusion on surfaces is an elegant way of probing adsorbate–substrate interactions, with the potential to deliver a diffusion potential energy surface [1–5]. Cold neutrons and helium atoms have been tested as probes for analyzing molecule dynamics on surfaces quite early in the history of surface science [6, 7]. Recent upgrades of cold neutron spectrometers [8–13] and the creation of novel helium scattering spectrometers [14] have promoted them to well suited tools for surface diffusion studies [4, 15–23]. Their dynamical window of about $10^{-12} \sim 10^{-6}$ s and their spatial resolution at the atomic scale, covers the typical time–space window of diffusing molecules at technically interesting temperatures [6, 8, 24–27].

Substantial recent improvements of molecular dynamics (MD) simulation software and the easy access to fast computing facilities provide an important complement to the study of diffusion by means of spectroscopy. Indeed, simulations often provide the key for the interpretation of the experimental data, since the experimental data alone do often not allow a unique interpretation [28–31]. In addition, the usefulness of scattering techniques in diffusion studies depends heavily on the availability of an *analytical* theoretical framework that relates diffusion mechanisms to their respective signatures in the measured scattering functions [3, 26, 32, 33]. The Van Hove formalism of correlation functions [34] provides a solid framework within which we can develop analytical models for particular systems [24–26, 35]. Fourier transformations in time–energy and in space, respectively, connect the experimental data, i.e., the scattering functions, $S(\mathbf{Q}, \omega)$ and $I(\mathbf{Q}, t)$, with the pair correlation function, $G(\mathbf{r}, t)$, and, hence, with the dynamics of the system: the probability of finding a particle in a given position at a certain time [34].

In this paper, we develop the incoherent scattering law for a system of disk like molecules with a six-fold point symmetry adsorbed on a hexagonal surface lattice. Nowadays, the discovery of astonishing mechanical and electronic properties of graphitic systems [36, 37] turns them into very interesting substrates on which to probe molecular diffusion. This model will allow for a deeper understanding of the diffusion of benzene molecule on basal plane graphite surfaces which has been measured in recent helium and neutron spectroscopy experiments [23, 38]. Although the theoretical neutron scattering laws for a molecule undergoing continuous translations [25, 26], continuous rotations [6, 39] or jump diffusive rotations [40, 41] have already been developed many times, this is the first time to our knowledge that the complete scattering law holding all this contributions together has being obtained.

This paper is organized as follows: In the first part, the general theory of the neutron differential scattering cross-section is presented. Then, we will focus on the particular case of the benzene system. We will discuss the different types of motions that we expect when molecules are lying flat on the surface: translations, free rotations and jump rotations. We will deduce the scattering function arising from this combination

of dynamical process. Finally, the scattering function for the particular case of a two dimensional powder sample is calculated, in order to make the model suitable for experiments performed with exfoliated graphite substrates. We will finish with a summary of the main results and discuss possible future improvements and applications of the model.

2. Derivation of the scattering functions

2.1. General properties of the neutron scattering function

We start our derivation with the double differential scattering cross section of a system made of N' identical particles, without loss of generality [35]:

$$\frac{d^2\sigma}{d\Omega d\omega} = \frac{k}{k_0}\frac{N'}{4\pi}\left[\sigma_{coh}S_{coh}(\mathbf{Q},\omega) + \sigma_{inc}S_{inc}(\mathbf{Q},\omega)\right]. \tag{1}$$

Here, Ω is the scattering solid angle, $\hbar\omega$ and $\mathbf{Q}$ are the energy and momentum transfer upon scattering, respectively, and k_0 and k are the respective wave-numbers of the neutron before and after scattering. In the formulation of Eq. 1, the right-hand-side is already split up in coherent, $S_{coh}(\mathbf{Q},\omega)$, and incoherent, $S_{inc}(\mathbf{Q},\omega)$, scattering functions. In order to reduce the complexity of the model, we will focus on the incoherent part of the scattering. Indeed, the very large incoherent scattering cross section of hydrogen atoms turns them into the main neutron scatterers in a system composed by fully hydrogenated benzene molecules (see table 1 and reference [42]). Thus, the scattering

Table 1. Incoherent and coherent scattering cross-sections of hydrogen and carbon atoms [25].

σ [barn]	H	C
σ_{inc}	80.26	0.0005
σ_{coh}	1.75	5.564

cross section reduces to:

$$\frac{d^2\sigma}{d\Omega d\omega} \simeq \frac{k}{k_0}\frac{N'}{4\pi}\sigma_{inc}S_{inc}(\mathbf{Q},\omega) = \frac{k}{k_0}\frac{N'}{4\pi}\frac{\sigma_{inc}}{2\pi\hbar}\int I_{inc}(\mathbf{Q},t)\exp(-i\omega t)dt, \tag{2}$$

where

$$I_{inc}(\mathbf{Q},t) = \frac{1}{N'}\sum_{j}^{N'}\langle\exp(-i\mathbf{Q}\cdot\mathbf{r}_j(t))\exp(i\mathbf{Q}\cdot\mathbf{r}_j(0))\rangle \tag{3}$$

is the so-called *intermediate scattering function, ISF*. This function can be factorized in terms of the center of mass motion and the single atom motion in the molecule by splitting the position vector of the j-th atom belonging to the γ-th molecule:

$$\mathbf{r}_j = \mathbf{R}_\gamma + \mathbf{r}_{\gamma j}, \tag{4}$$

where $\mathbf{R}_\gamma$ is the position of the center-of-mass with respect to the laboratory spatial frame and $\mathbf{r}_{j\gamma}$ refers to the atomic positions with respect to the molecular frame of reference. Equation 3 reads now:

$$I_{inc}(\mathbf{Q},t) = \frac{1}{N'}\sum_{\gamma}^{N}\sum_{j}^{6}\langle \exp[-i\mathbf{Q}\cdot(\mathbf{R}_\gamma(t)+\mathbf{r}_{\gamma j}(t))]\exp[i\mathbf{Q}\cdot(\mathbf{R}_\gamma(0)+\mathbf{r}_{\gamma j}(0))]\rangle, \quad (5)$$

where N' is the total number of (hydrogen) atoms and N is the total number of molecules. Since the molecule of benzene contains six hydrogen atoms: $N' = 6N$. Within the *weak hindered approximation* [42], we neglect statistical correlations between: (i) the rotational and the translational motion of one molecule and (ii) the rotational motion of different molecules. As a result, we can separate the center-of-mass contribution from the single atom part:

$$I_{inc}(\mathbf{Q},t) = \frac{1}{N'}\left[\sum_{\gamma}^{N} F_s^\gamma(\mathbf{Q},t)\right]\left[\sum_{j}^{6} Y_j^\gamma(\mathbf{Q},t)\right], \quad (6)$$

where the following functions describing the molecular center-of-mass motion [43]:

$$F_s^\gamma(\mathbf{Q},t) = \langle \exp[-i\mathbf{Q}\cdot\mathbf{R}_\gamma(t)]\exp[i\mathbf{Q}\cdot\mathbf{R}_\gamma(0)]\rangle, \quad (7)$$

and the single atom dynamics [43]:

$$Y_j^\gamma(\mathbf{Q},t) = \langle \exp[-i\mathbf{Q}\cdot\mathbf{r}_{\gamma j}(t)]\exp[i\mathbf{Q}\cdot\mathbf{r}_{\gamma j}(0)]\rangle. \quad (8)$$

are used.

2.2. Translational part: center-of-mass dynamics

The *translational* part of the ISF in Eq. 6 is represented by the center of mass motion, $F_s^\gamma(\mathbf{Q},t)$. Within the classical mechanics framework, the averaged trajectories give rise to the following translational ISF [44]:

$$\begin{aligned} F_s^\gamma(\mathbf{Q},t) &= \langle \exp\left[-i\mathbf{Q}\cdot\mathbf{R}_\gamma(t)\right]\exp\left[i\mathbf{Q}\cdot\mathbf{R}_\gamma(0)\right]\rangle \\ &= \langle \exp\left[i\mathbf{Q}\cdot\mathbf{R}_\gamma(0)-\mathbf{R}_\gamma(t)\right]\rangle \\ &= \langle \exp\left[i\mathbf{Q}\cdot\textstyle\int_0^t \widehat{v}_{\mathbf{Q}}^\gamma(t')dt'\right]\rangle, \end{aligned} \quad (9)$$

where $\widehat{v}_{\mathbf{Q}}^\gamma(t')$ is the averaged velocity of a single molecule for a given direction in the Q-space. Martínez-Casado *et al.* [44,45] have shown that the substrate and the surrounding adparticles can be modelled as two independent and uncorrelated thermal baths in which the adparticle under consideration is moving: *the two-bath model*. This two bath model description has been confirmed by experiment [23] leading to two contributions for the friction coefficient: the substrate friction and the collisional friction. Since the dynamic of the system is completely driven by temperature, we can assume that all the molecules have the same averaged velocity. As a result, the dependence on a specific molecule (labeled with index γ) of the terms in the summation of Eq. 6 vanishes and the summation is reduced to:

$$\sum_{\gamma}^{N} F_s^\gamma(\mathbf{Q},t) = NF_s(\mathbf{Q},t), \quad (10)$$

where N is the total number of benzene molecules in the system and $F_s(\mathbf{Q},t)$ is the *generalized translational ISF* for a single adparticle (the adsorbed benzene molecule reduced to its center-of-mass):

$$F_s(\mathbf{Q},t) = \langle \exp(i\mathbf{Q}\cdot\int_0^t \widehat{v}_{\mathbf{Q}}(t')dt')\rangle. \tag{11}$$

In the case of benzene–graphite, the potential energy due to the molecule–substrate interaction is negligible in comparison to the thermal energy of the system [23]. Thus, the adparticle has *quasi-free 2 dimensional dynamics* and moves on an almost flat potential [44]. Two important consequences are deduced. First of all, the adparticle motion is only influenced by stochastic forces [44]. Within this regime, *the Gaussian approximation* holds [44] and provides:

$$F_s(\mathbf{Q},t) \backsimeq \exp(-\mathbf{Q}^2\int_0^t (t-t')C_v(t')dt'), \tag{12}$$

where $C_v(t)$ is the velocity autocorrelation function:

$$C_v(t) = \langle v_{\mathbf{Q}}(t)v_{\mathbf{Q}}(0)\rangle. \tag{13}$$

Secondly, a flat potential energy surface implies that all directions are equally affordable from an energetic point of view. Therefore, the autocorrelation function is *isotropic*. These two arguments provide the following autocorrelation function:

$$C_v(t) = \frac{k_BT}{m}\exp(-\eta t), \tag{14}$$

with m being the benzene mass when the whole molecule is reduced to its center-of-mass, and η being the *translational friction parameter*, which contains the two aforementioned contributions [44, 45]: the substrate friction arising from the energy exchange between the substrate and the adparticle and the collisional friction due to the energy exchange between the adparticles. All these considerations yield the full ISF for translations [44]:

$$\begin{aligned} F_s(\mathbf{Q},t) &= \exp[-\chi^2(e^{-\eta t}+\eta t-1)] \\ &= \exp[\chi^2]\textstyle\sum_{n=0}^{\infty}\frac{\chi^{2n}}{n!}\exp[-(n+\chi^2)\eta t], \end{aligned} \tag{15}$$

as an exponential function which can be expanded in terms of a summation of single exponential decays. Its corresponding scattering law is a summation of Lorentzian functions where each quasi-elastic broadening, Γ_n, is given by:

$$\Gamma_n = (n+\chi^2)\eta. \tag{16}$$

In the two thermal baths model, the *substrate bath* results from the creation and annihilation of virtual surface phonons as well as virtual excitations of low-lying frequency modes of the adparticle and gives rise to the dependence on the index n. The χ^2 parameter is the so-called *shape parameter* [44] which is given by:

$$\chi^2(\mathbf{Q}) \equiv \frac{k_BT}{m}\frac{\mathbf{Q}^2}{\eta^2} = \frac{\langle v_0^2\rangle\mathbf{Q}^2}{\eta^2}. \tag{17}$$

In the high friction regime, the ISF tends to a single exponential decay in time (diffusive regime):

$$\eta \gg 1 \Rightarrow \chi^2 \ll 1, \chi^2\eta \ll 1 \Rightarrow F_s(\mathbf{Q},t) \simeq \exp[-2\chi^2\eta t], \tag{18}$$

while in the low friction regime, the ISF becomes a Gaussian function of time, independent of friction:

$$\eta \ll 1 \Rightarrow \chi^2 \gg 1, \chi^2\eta \gg 1 \Rightarrow F_s(\mathbf{Q},t) \simeq \exp\left[-\frac{1}{2}\langle v_0^2\rangle Q^2 t^2\right], \tag{19}$$

which is the typical signature of ballistic diffusion [26]. Due to the isotropy of the flat potential energy surface, no favored direction exists and the friction parameter η is isotropic. The shape parameter is then:

$$\chi^2(Q) = \frac{\langle v_0^2\rangle}{\eta^2}Q^2, \tag{20}$$

and F_s depends only on the square modulus of the momentum transfer vector: $|\mathbf{Q}|^2 = Q^2$. Furthermore, the mean square velocity $\langle v_0^2\rangle$ is related to the mean free path $\tilde{l}$ and the *self-diffusion* coefficient D by [44]:

$$\begin{cases} \tilde{l} \equiv \tau\sqrt{\langle v_0^2\rangle} \\ \qquad\qquad\quad \Rightarrow \langle v_0^2\rangle = \left(\frac{D}{\tilde{l}}\right)^2 \\ D \equiv \tau\langle v_0^2\rangle. \end{cases} \tag{21}$$

Hedgeland *et al.* [23] provided experimental values for the mean free path, $\tilde{l} \sim 0.7$ Å, and for the diffusion coefficient, $D = 5.39(\pm 0.13) \times 10^{-9}$ m^{2}s^{-1}, of deuterated benzene adsorbed on the basal plane of graphite substrates at a surface temperature of 140 K. This leads to a mean square velocity of $\langle v_0^2\rangle \sim 5.9 \times 10^3$ m^{2}s^{-2}. However, these values should be carefully adapted for the case of the hydrogenated benzene. Indeed, the incoherent scattering (h-benzene) probes the self-correlation function: single molecule motion. Conversely the coherent scattering (d-benzene) comes from the collective motion of molecules: clusters. But if single molecules are trapped into clusters undergoing translations, the coherent and the incoherent scattering arise from the same scattering mechanism: the translational motion. So, in principle, the experimental values for d-benzene are a good benchmark for the center of mass h-benzene data analysis.

2.3. Rotational part

The rotational part of the ISF describes two apparently incompatible diffusive behaviors, but which have been observed in experiments and in MD simulations. On one side, the measured activation energy for diffusion of 17 meV [23], is low in comparison to the thermal energy at 140 K (12 meV). Thus, the data presented in ref. [23] clearly show Brownian diffusion without a trace of jump diffusion. Conversely, MD simulations reveal a marked dependence of the diffusion coefficient on coverage [28]. Furthermore, measurements on hydrogenated benzene are better described by the Chudley-Elliott model for jump diffusion than by the pure Brownian model [46].

In order to embody the aforementioned features into a unique function, we consider the *total single particle ISF* $Y_j(\mathbf{Q},t)$ in Eq. 6 as the product of two functions:

$$Y_j(\mathbf{Q},t) = Y_j^{free}(\mathbf{Q},t)Y_j^{jump}(\mathbf{Q},t) \tag{22}$$

where $Y_j^{free}(\mathbf{Q},t)$ comes from the free rotational diffusion and $Y_j^{jump}(\mathbf{Q},t)$ describes the jump diffusion part.

Free rotational diffusion, $Y_j^{free}(\mathbf{Q},t)$: In the case of a weak interaction potential between the adsorbate and the substrate, as observed for benzene–graphite [28], free molecules (not surrounded by neighboring molecules) can rotate without feeling any substantial energy barrier. In this section we deduce the ISF arising from a single atom that is part of a freely rotating molecule. Starting from the definition of $Y_j(\mathbf{Q},t)$ in Eq. 8, the averages by means of orientation probability distribution functions can be evaluated.

If a Boltzman distribution of the initial orientations of the j-th atom in the molecule is assumed

$$p(\Omega_j(0)) = \frac{1}{Z}\exp\left[\frac{-E(\Omega_j(0))}{k_BT}\right], \tag{23}$$

where $E(\Omega_j(0))$ is the energy associated with each initial orientation, $\Omega_j(0)$, k_B is the Boltzmann constant, T is the surface temperature and $Z = \int_0^{2\pi} d\Omega_j(0) exp[-E(\Omega_j(0))/k_BT]$ is the partition function, then for a top symmetric molecule, like benzene lying flat on the surface, $p(\Omega_j(0))$ is isotropic on the surface [42]. This means that the energy E in Eq. 23 does not depend on $\Omega_j(0)$ and $p(\Omega_j(0))$ is a constant:

$$p = \frac{1}{2\pi}. \tag{24}$$

For describing the averaged orientations at a posterior time, t, we define the rotational correlation function $G(\Omega_j, \Omega_j(0), t)$, that is, the probability of finding the j-th nucleus in the molecule oriented in direction Ω_j at time t, if this very same nucleus lied in the direction $\Omega_j(0)$ at time $t = 0$ [42]. G_s satisfies *the master equation for rotational diffusion* (the equivalent of Fick's law in translational diffusion) [39,42], which is defined in general terms as:

$$\frac{\partial}{\partial t}G_s(\Omega_j, \Omega_j(0), t) = D_r \Delta G_s(\Omega_j, \Omega_j(0), t), \tag{25}$$

where Δ is the *Laplacian operator* in the corresponding coordinates. According to its definition, G_s is a δ-function at $t = 0$:

$$G_s(\Omega_j, \Omega_j(0), 0) = \delta(\Omega_j - \Omega_j(0)). \tag{26}$$

Planar rotations are described by a cylindrical Laplacian with a single degree of freedom, the azimuthal angle, ϕ, because the atoms are moving on a circle (one dimensional

motion). Hence, the direction of the j-th atom, Ω_j, is equivalent to ϕ_j and the master equation becomes [39]:

$$\frac{\partial}{\partial t}G_s(\phi_j,\phi_j(0),t) = D_r\frac{1}{\rho^2}\frac{\partial^2}{\partial\phi_j^2}G_s(\phi_j,\phi_j(0),t), \tag{27}$$

where D_r is the *diffusion coefficient for rotations*. Its exact meaning is discussed in reference [39]. It is defined in analogy to the translational diffusion coefficient that was deduced by Einstein for his theory on Brownian motion:

$$D_r = \frac{k_B T}{I\eta_R}, \tag{28}$$

where I is the moment of inertia of the rotating molecule with respect to its sixfold symmetry axis. η_R is the *rotational friction parameter* and ρ is the radius of the circle on which the atoms move (see Fig. 1). Solutions of Eq. 27 are found by expanding G_s in terms of eigenfunctions of the operator $D_r\frac{1}{\rho^2}\frac{\partial^2}{\partial\phi_j^2}$ [39, 42]:

$$\psi_n(\phi_j,\phi_j(0),t) = \frac{1}{\sqrt{2\pi}}e^{in(\phi_j-\phi_j(0))}F_n(t), \tag{29}$$

where $F_n(t)$ are the so-called *relaxation functions* and bear the time dependence. Since the initial conditions for G_s in Eq. 26 must hold for the ψ_n functions as well, then,

$$F_n(0) = 1. \tag{30}$$

By solving the master Eq. 27 for the ψ_n functions:

$$\frac{\partial}{\partial t}\psi_n(\phi_j,\phi_j(0)) = D_r\frac{1}{\rho^2}\frac{\partial^2}{\partial\phi_j^2}\psi_n(\phi_j,\phi_j(0),t), \tag{31}$$

the analytical expression of the relaxation functions can be expressed as

$$F_n(t) = \exp\left[-D_r\frac{n^2}{\rho^2}t\right]. \tag{32}$$

G_s can now be obtained as the linear combination of such a complete set of eigenfunctions [39]:

$$G_s(\phi_j,\phi_j(0),t) = \frac{1}{2\pi}\sum_{n=-\infty}^{\infty}e^{in[\phi_j-\phi_j(0)]}\exp\left(-D_r\frac{n^2}{\rho^2}t\right). \tag{33}$$

Then ISF can be calculated from

$$Y_j^{free}(\mathbf{Q},t) = \int p(\Omega_j(0))\exp(i\mathbf{Q}\cdot\mathbf{r}_j(0))I_s(\mathbf{Q},\Omega_j(0),t)d\Omega_j(0), \tag{34}$$

where we define:

$$I_s(\mathbf{Q},\Omega_j(0),t) \equiv \int \exp(-i\mathbf{Q}\cdot\mathbf{r}_j(t))G_s(\Omega_j,\Omega_j(0),t)d\Omega_j. \tag{35}$$

We consider that the incoming and outgoing wave vectors $\mathbf{k}_0$ and $\mathbf{k}$, respectively, lie in the plane of the molecules (see right panel in Fig. 1). In this case the momentum transfer vector, $\mathbf{Q}$, will also lie in the molecular plane. As a consequence we find:

$$\exp(-i\mathbf{Q}\cdot\mathbf{r_j}(t)) = \exp[-iQ\rho\cos(\phi_j(t)-\alpha)]. \tag{36}$$

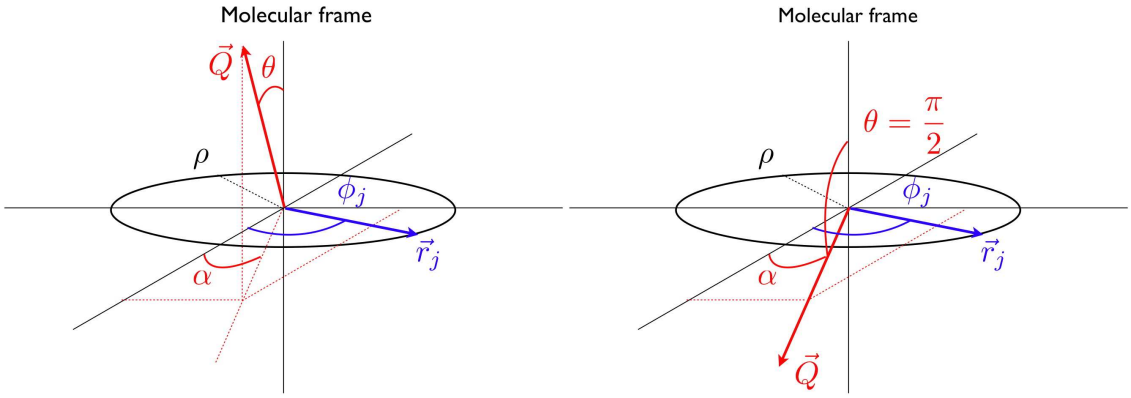

Figure 1. Left panel: Geometry of the scattering for a generic momentum transfer vector. The red vector represents the momentum transfer vector **Q** and the blue vector represents the position of the j-th scatterer nucleus in the molecule with respect to the molecular frame. The black circle depicts protons trajectory in a rotating benzene molecule. The polar angles in the molecular frame θ, α (for **Q**) and ϕ_j (for the j-th proton) are indicated. **Right panel**: Geometry of the scattering for a momentum transfer vector within the molecular plane (xy axis). In this case $\theta = \pi/2$. Our experimental geometry corresponds to the right panel.

It is useful to expand equation 36 in terms of Bessel functions [47]:

$$\exp[-iQ\rho\cos(\phi_j(t)-\alpha)] = \sum_{l=-\infty}^{\infty} i^l J_l(-Q\rho)e^{il(\phi_j(t)-\alpha)} \tag{37}$$

$$= \sum_{l=-\infty}^{\infty} (-i)^l J_l(Q\rho)e^{il(\phi_j(t)-\alpha)}, \tag{38}$$

where Q is the modulus of the momentum transfer vector, **Q**, and ρ is the modulus of $\mathbf{r}_j$ which corresponds to the radius of the circular trajectories of the moving atoms (see Fig. 1). Equations 33 and 38 lead to:

$$I_s(\mathbf{Q},\phi_j(0),t) = \sum_{n=-\infty}^{\infty} (-i)^n J_n(Q\rho)e^{in(\phi_j(0)-\alpha)} \exp\left(-\frac{n^2}{\rho^2}D_r t\right). \tag{39}$$

Applying the expansion 38 to $\exp(-i\mathbf{Q}\cdot\mathbf{r_j}(0))$ and the isotropic form of $p(\phi_j(0))$ (Eq. 24), yield the final intermediate scattering function for free rotations:

$$Y^{free}(Q,t) = \sum_{l=-\infty}^{\infty} J_l^2(Q\rho)\exp\left(-\frac{l^2}{\rho^2}D_r t\right). \tag{40}$$

As expected [6,39], $Y^{free}(\mathbf{Q},t)$ is the summation of exponential decays in time and does not depend anymore on the angle α nor on the index j. The integration over all the initial orientations removes its dependency on the position of the specific nucleus. As a

result we obtain the generic ISF of a nucleus (no matter which one) in a freely rotating benzene molecule.

Rotational jump diffusion: As we have already stated, the interaction between adsorbate and substrate in the benzene–graphite system is too weak [23, 28] to prevent an isolated molecule to move continuously on an almost flat potential energy surface. However, the substrate has a second order effect, which is significantly enhanced with coverage [28]. Since in our model the substrate and the adsorbed molecules share the same hexagonal symmetry, the former can impose a preferential orientation for adsorption to the ad-layer. In addition, the "cog wheel" shape of hexagonal molecules allows them to get locked into each other when they cluster. As a result, the orientation of all the molecules in a cluster is fixed by the surface geometry, and their motion (reorientation around their six-fold symmetry axis, i.e planar rotations) is strongly hindered. MD simulations [28] show how the height of the energy barrier for diffusion of benzene–graphite is amplified with increasing coverage. We can observe a transition from a continuous diffusive regime (isolated molecules) towards a jump diffusive regime (clusters) [46]. In this section we use the Chudley-Elliott model for finding an analytical expression of $Y_j^{jump[}(\mathbf{Q},t)$, the ISF arising from jump rotation effects.

In the original Chudley-Elliott model for jump diffusion, the master equation which describes the time evolution of the probability of finding a proton in a certain position, $P(\mathbf{r},t)$, is [26]:

$$\frac{\partial}{\partial t}P(\mathbf{r},t) = \frac{1}{n}\sum_m \frac{1}{\tau_m}\left[P(\mathbf{r}+\mathbf{l}_m,t) - P(\mathbf{r},t)\right], \tag{41}$$

where $\mathbf{r}$ is the position of one proton, $\mathbf{l}_m$ is the jump vector to the m-th neighbour site, τ_m is the residence time of the proton in the m-th site and n is the total number of available sites from an initial position. Fourier transforming Eq. 41 in space is obtained:

$$\begin{aligned}\tfrac{\partial}{\partial t}\textstyle\int d\mathbf{r}\exp(i\mathbf{Q}\cdot\mathbf{r})P(\mathbf{r},t) \;&= \tfrac{1}{n}\textstyle\sum_m^n \tfrac{1}{\tau_m}[\exp(-i\mathbf{Q}\cdot\mathbf{l}_m)\\ &\times \textstyle\int d\mathbf{r}\exp(i\mathbf{Q}\cdot\mathbf{r})P(\mathbf{r},t)\\ &- \textstyle\int d\mathbf{r}\exp(i\mathbf{Q}\cdot\mathbf{r})P(\mathbf{r},t)].\end{aligned} \tag{42}$$

If we now define:

$$f(\mathbf{Q},t) \equiv \int d\mathbf{r}\exp(i\mathbf{Q}\cdot\mathbf{r})P(\mathbf{r},t) \tag{43}$$

and introduce it in Eq. 42, we obtain a simplified rate equation:

$$\frac{\partial}{\partial t}f(\mathbf{Q},t) = \frac{1}{n}\left[\sum_m^n \frac{1}{\tau_m}\exp(-i\mathbf{Q}\cdot\mathbf{l}_m) - 1\right] f(\mathbf{Q},t), \tag{44}$$

which is easily solved and gives an exponential decay:

$$f(\mathbf{Q},t) = f(\mathbf{Q},0)\exp[-M(\mathbf{Q})t], \tag{45}$$

where the inverse time constant is:

$$M(\mathbf{Q}) \equiv -\frac{1}{n}\frac{1}{\tau}\left[\sum_m^n \exp(-i\mathbf{Q}\cdot\mathbf{l}_m) - 1\right]. \tag{46}$$

Assuming that the j-th atom sits in $\mathbf{r}_k(0)$ at $t = 0$, Fig. 2 shows all the possible jumps associated with different rotations of angle $k\pi/3$ around the molecule's sixfold symmetry axis. In this case, the self-correlation function of the j-th proton, $G_s(\mathbf{r}_j, t)$,

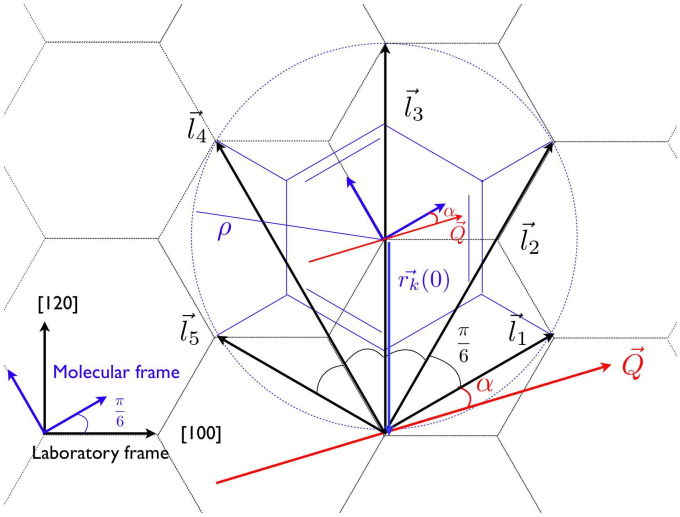

Figure 2. Without loss of generality we assume the equilibrium adsorption site similar to the one established for a benzene molecule on a graphite layer as described in reference [28]. The figure describes the different jumps that a single atom in a given initial position can perform during rotations. Red arrows show the direction of the momentum transfer vector, $\mathbf{Q}$, which forms an arbitrary angle α with the first jump vector.

is the average over all the possible initial positions of the probability function $P(\mathbf{r}, t)$ defined above in Eq. 41. The particularity of jump rotations with respect to jumps on Bravais lattices, is that not all the starting points are equivalent. This is due to geometrical reasons. Therefore, we cannot simply identify $G_s(\mathbf{r}_j, t)$ with $P(\mathbf{r}, t)$ and Y_j^{jump} with $f(\mathbf{Q}, t)$ in Eqs. 41 and 45, but we need to perform the average over all the initial positions. The rate equation reads then:

$$\frac{\partial}{\partial t} G_s(\mathbf{r}_j, t) \; = \frac{1}{n^2} \sum_m^n \sum_k^n \frac{1}{\tau_m} \left[G_s(\mathbf{r}_j + \mathbf{l}_{mk}, t) - G_s(\mathbf{r}_j, t) \right], \tag{47}$$

where k runs over all initial positions and m over all final sites. The Fourier transform in space gives rise to:

$$\frac{\partial}{\partial t} Y_j^{jump}(\mathbf{Q}, t) = \frac{1}{n^2} \left[\sum_m^n \sum_k^n \frac{1}{\tau_m} \exp(-i\mathbf{Q} \cdot \mathbf{l}_{mk}) - 1 \right] Y_j^{jump}(\mathbf{Q}, t) \tag{48}$$

where we have applied the standard definition of the ISF [34]:

$$Y_j^{jump}(\mathbf{Q}, t) = (2\pi)^3 \int G_s(\mathbf{r}_j, t) \exp(i\mathbf{Q} \cdot \mathbf{r}_j) d\mathbf{r}_j. \tag{49}$$

Since the indexes m and k run over all the $n = 6$ sites in the molecule, we end up with a complete set of $n^2 = 36$ jump vectors (see Fig. 3). Due to the geometry of the molecule,

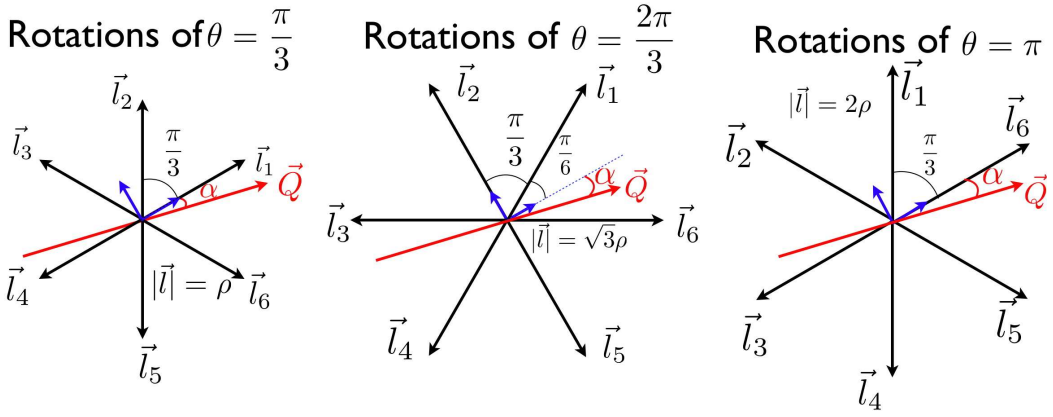

Figure 3. All the different jump vectors $\mathbf{l_{km}}$ arising from rotations of angles spanning from $k\pi/3$ to π from different starting positions. Rotations of angle from $-\frac{\pi}{3}$ to $-\pi$ will give rise to exactly the same set of jump vectors.

rotations of $k\pi/3+\pi$ radians will give rise to the same contribution as rotations of $k\pi/3$ radians. The summation thus reduces to $\pi/3$, $2\pi/3$ and π rotations. The solution of Eq. 48 is still a single exponential decay:

$$Y_j^{jump}(\mathbf{Q},t) = Y_j^{jump}(\mathbf{Q},0)\exp[-M(\mathbf{Q})t]. \tag{50}$$

where the inverse time constant is

$$M(\mathbf{Q}) = -\frac{1}{18}\frac{1}{\tau}\sum_{k=1}^{6}\sum_{l=1}^{3}\left\{\exp\left[-iQc_l\rho\cos\left(\alpha+\theta_{kl}\right)\right]-1\right\}, \tag{51}$$

and the phase θ_{kl}

$$\theta_{kl} = (l-1)\frac{\pi}{6} + (k-1)\frac{\pi}{3}. \tag{52}$$

The factor c_l gives the effective jump length for each kind of rotation of the molecule around its six-fold symmetry axis: $c_1 = 1$ for a $\pi/3$ radians rotation, $c_2 = \sqrt{3}$ for a $2\pi/3$ radians rotation and $c_3 = 2$ for a π radians rotation. For simplicity we have assumed that all the jumps have the same probability, $1/\tau$, but this is only true for high temperatures and low coverages. Finally, since at $t = 0$, $G_s(\mathbf{r}_j, 0) = \delta(\mathbf{r}_j)$ [34], we find that $Y_j^{jump}(\mathbf{Q}, 0) = 1$. Again, we obtain an ISF which is independent of a specific atom in the molecule.

We are now ready to write the *complete rotational ISF for a single atom* as:

$$Y(\mathbf{Q},t) = \exp[-M(\mathbf{Q})t]\sum_{l=-\infty}^{\infty} J_l^2(Q\rho)\exp\left(-\frac{l^2}{\rho^2}D_r t\right) \tag{53}$$

The dependence on the index j drops and we obtain a generalized ISF, which holds for all atoms in the molecule. This yields:

$$\sum_j^6 Y_j(\mathbf{Q},t) = 6Y(\mathbf{Q},t) \tag{54}$$

2.4. Total intermediate scattering function, scattering function and differential cross-section

Introducing now the center-of-mass ISF (Eq. 12) and the single atom ISF (eq. 54) into Eq. 6, *the total ISF for a system of N benzene molecules* is written as:

$$I_{inc} = \frac{N}{N'} F_s(\mathbf{Q},t) 6 Y(\mathbf{Q},t) = F_s(\mathbf{Q},t) Y(\mathbf{Q},t). \tag{55}$$

The analytical expression of the two previous functions provides:

$$I_{inc}(\mathbf{Q},t) = \sum_{n=0}^{\infty} \sum_{l=-\infty}^{\infty} A_{nl}(Q) \exp\left[-\Gamma_{nl}(\mathbf{Q}) t\right], \tag{56}$$

which is a summation of exponential decays. Each term is weighed by an amplitude depending on the geometry of the free rotations (see Fig. 4) and the translational motion:

$$A_{nl}(Q) = \frac{1}{n!} \left(\frac{-\langle v_0^2 \rangle}{\eta^2} \right)^n J_l^2(Q\rho) \exp\left(\frac{\langle v_0^2 \rangle}{\eta^2} Q^2 \right) Q^{2n}, \tag{57}$$

and with a total inverse time constant, which is the sum of all the contributions to the dynamics :

$$\Gamma_{nl}(\mathbf{Q}) = \eta n + \frac{l^2}{\rho^2} D_r + \frac{\langle v_0^2 \rangle}{\eta} Q^2 + M(\mathbf{Q}). \tag{58}$$

Free rotations and the part of translations related to the phonon friction do not display any dependence on the momentum transfer $\mathbf{Q}$. They simply add a constant offset which increases for higher terms in the summation with indexes n and l. Thus, dependence on $\mathbf{Q}$ comes namely from the Brownian part of translations and from the jump rotations inside clusters. However, experimental neutron spectroscopy data are mostly yielding *the scattering function* $S(\mathbf{Q},\omega)$. The Fourier transform of Eq. 56 in time provides, as expected, a summation of Lorentzian functions:

$$S_{inc}(\mathbf{Q},\omega) = \frac{1}{2\pi\hbar} \sum_{n=0}^{\infty} \sum_{l=-\infty}^{\infty} A_{nl}(Q) \frac{\Gamma_{nl}(\mathbf{Q})}{\Gamma_{nl}^2(\mathbf{Q}) + \omega^2}, \tag{59}$$

whose HWHM is the inverse time constant Γ_{nl}, also known as the *quasi-elastic broadening* in the energy domain. Finally, the differential cross-section is obtained by the substitution of Eq. 59 into Eq. 2:

$$\frac{d^2\sigma}{\partial\Omega\partial\Delta E}(\mathbf{Q},\Delta E) = \frac{k}{k_0} \frac{N}{2\pi\hbar} \frac{\sigma_{inc}}{4\pi} \sum_{n=0}^{\infty} \sum_{l=-\infty}^{\infty} A_{nl}(Q) \frac{\hbar\Gamma_{nl}(\mathbf{Q})}{\hbar^2\Gamma_{nl}^2(\mathbf{Q}) + \Delta E^2}. \tag{60}$$

2.5. Two-dimensional powder sample case: the exfoliated graphite substrate

To fully adapt the model to the case of exfoliated graphite surfaces, the two dimensional powder case need to be considered. In this kind of substrates, the basal planes of the graphite micro-crystals are oriented randomly within the plane parallel to the macroscopic surface [48]. Consequently, the differential cross-section results from the contribution of all the micro-crystals, averaged over all the possible orientations within

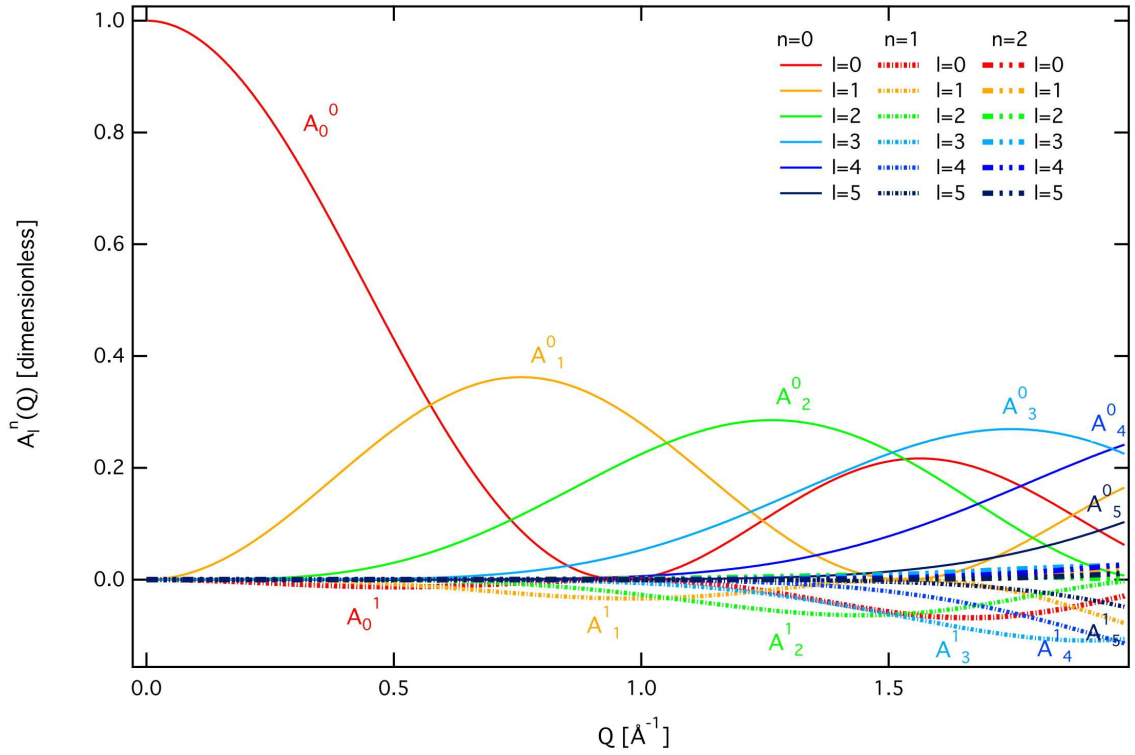

Figure 4. Representation of functions A_l^n, defined in Eq. 57, for different parameters of indexes n and l.

the plane. Assuming an isotropic orientation of the graphite micro-crystals the resulting neutron differential cross-section is:

$$\frac{d^2\sigma}{d\Omega d\omega}(Q,\Delta E) = \langle \frac{d^2\sigma}{d\Omega d\omega}(\mathbf{Q},\Delta E)\rangle_\alpha = \frac{1}{2\pi}\int_0^{2\pi} d\alpha \frac{d^2\sigma}{d\Omega d\omega}(\mathbf{Q},\Delta E), \qquad (61)$$

where α is the angle formed by the momentum transfer and the molecule (see Fig. 2). The Fourier transformation in time relates the differential cross-section to the ISF (see Eq. 2), so we can perform the integration on the ISF, which – being a summation of exponential functions – is much easier to handle:

$$I_{inc}(Q,t) = \sum_{n=0}^{\infty}\sum_{l=-\infty}^{\infty} \frac{1}{2\pi}\int_0^{2\pi} A_{nl}(Q)\exp\left[-\Gamma_{nl}(\mathbf{Q})t\right] d\alpha. \qquad (62)$$

Since only the quasi-elastic broadening arising from molecules rotating in clusters, $M(\mathbf{Q})$, depends on vector $\mathbf{Q}$ (Eq. 58) the integral is reduced to:

$$\frac{1}{2\pi}\int_0^{2\pi} \exp\left[-M(\mathbf{Q})t\right] d\alpha = \exp\left\{\frac{1}{n}\frac{t}{\tau}\sum_{k=1}^{6}\sum_{l=1}^{3}\left[\exp\left(-iQc_l\rho\cos\left(\theta_{kl}\right)\right)-1\right]\right\}. \qquad (63)$$

The inverse time constant is then:

$$M(Q) = -\frac{1}{n}\frac{1}{\tau}\sum_{k=1}^{6}\sum_{l=1}^{3}\left[\exp\left(-iQc_l\rho\cos\left(\theta_{kl}\right)\right)-1\right] \qquad (64)$$

which can be written in a compact way as a summation of sinusoidal functions:

$$M(Q) = \frac{2}{9}\frac{1}{\tau}\left[2\sin^2\left(\frac{\rho Q}{4}\right) + 3\sin^2\left(\frac{\rho Q}{2}\right) + 2\sin^2\left(\frac{3\rho Q}{4}\right) + \sin^2\left(\rho Q\right)\right]. \quad (65)$$

The resulting integrated quasi-elastic broadening is shown in Fig. 5.

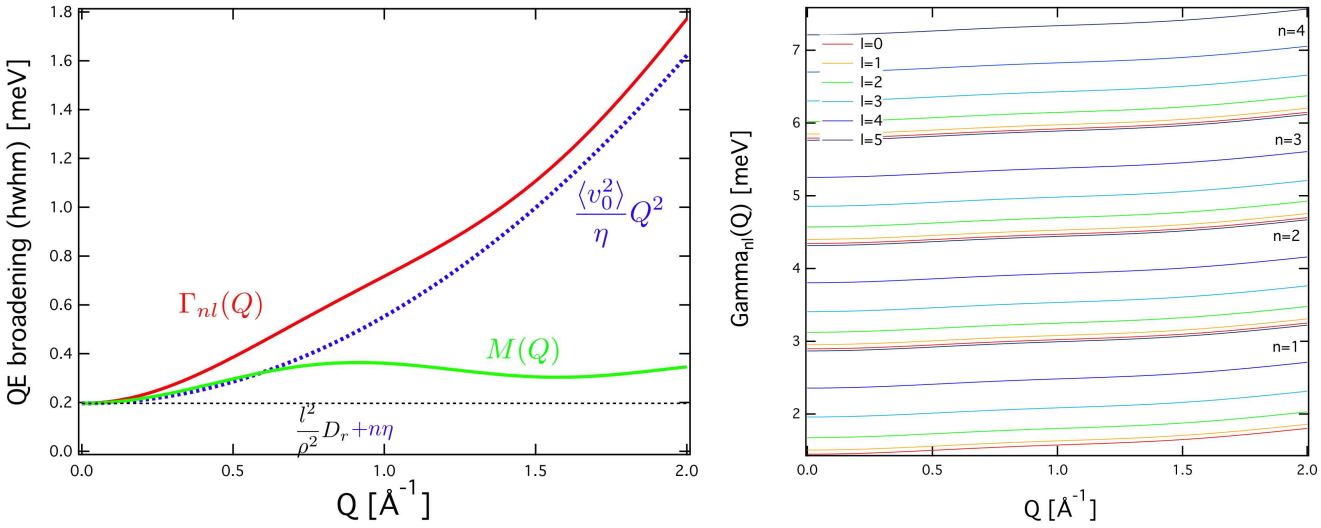

Figure 5. Representation of all the contributions to the quasi-elastic broadening Γ_{ln}, as defined in equation 58. **Left Panel:** n=0. **Right Panel** Quasi-elastic broadening for different indexes n and l.

2.6. Application of the model to experimental data

3. Conclusions

In this work we have developed a theoretical model for understanding the diffusive behavior of a system of molecules with a six-fold symmetry adsorbed on a flat hexagonal surface. The goal was to obtain an ISF, or through the time Fourier transform, the corresponding scattering law, resulting from the continuous diffusion of this molecules (related to translations of clusters and free rotations of isolated molecules) and the discontinuous diffusion due to molecules trapped within clusters. This theoretical description can be applied to experimental data arising from hydrogenated benzene adsorbed on the basal plane of graphite surfaces.

We have been inspired by the method of Sears for methane diffusion [6, 42, 43] based on the *weak hindered approximation* within which we assume the statistical independence of rotations and translations of a single molecule. This hypothesis allows the factorization of the intermediate scattering function in terms of the of center-of-mass and proton dynamics. The resulting ISF is a product of functions depending separately on the center-of-mass trajectories and the proton trajectories. Using the Van Hove formalism and more particularly the approaches given in ref. [44] for the translational

part, [42] for free rotations and [40] for the jump rotations within clusters, we have calculated the ISF using specific correlation functions for each dynamical process. As a result we obtain a summation of exponential decays in the time domain, or Lorentzian functions in the energy domain. The weight of each term is related to the geometry of the rotations and to the translational motion, while the quasi-elastic broadening is a sum of contributions arising from the different motions of the molecule. Finally we have calculated the specific ISF for a two dimensional powder sample. This is particularly useful when exfoliated graphite substrates are used in experiments.

The model we have developed can be seen as a first approximation to the problem of diffusion of molecules adsorbed on layers with the same symmetry. Indeed, special features can arise when the geometry of the ad-layer and the substrate is commensurate: the coupling between rotational and translational motion generates unexpected diffusive regimes that go well beyond the traditional models within the classical mechanics framework [49–51]. Since we have built our description within the framework of the weak hindered approximation, we have ignored such correlations, delivering a completely linear and classical model. Future work should consider the study of possible traces of quantum effects and non-linearity in the dynamics of systems sharing the same point geometry, such as benzene adsorbed on graphite substrates, in order to explore the possibility of non-linear diffusion and ballistic diffusion.

Acknowledgments

Support from the Ministerio de Ciencia e Innovacion (Spain) under project FIS2010-18132 is acknowledged. I. C.-A. acknowledges the Institut Laue-Langevin (France) for the funding of her PhD project and L. M. García-Vinuesa for its support at "Universidad de Zaragoza" (Spain).

References

[1] Tringides M C (ed) 1997 *Surface Diffusion: Atomistic and Collective Processes* (*NATO ASI series, Series B, Physics* vol 360) (New York: Plenum Press)
[2] Antczak G and Ehrlich G 2010 *Surface Diffusion: Metals, Metal Atoms, and Clusters* (Cambridge: Cambridge University Press)
[3] Miret-Artes S and Pollak E 2005 *J. Phys.: Condens. Matter* **17** S4133–S4150
[4] Jardine A P, Alexandrowicz G, Hedgeland H, Allison W and Ellis J 2009 *Phys. Chem. Chem. Phys.* **11** 3355–3374
[5] Fouquet P, Hedgeland H and Jardine A P 2010 *Z. Phys. Chem.* **224** 61–81
[6] Sears V F 1966 *Can. J. Phys.* **44** 1279 – 1297
[7] Doak R B and Toennies J P 1982 *Surface Science* **117** 1–12
[8] ILL 2008 *The Yellow Book 2008* (Grenoble: Institut Laue Langevin)
[9] Mason T E, Abernathy D, Anderson I, Ankner J, Egami T, Ehlers G, Ekkebus A, Granroth G, Hagen M, Herwig K, Hodges J, Hoffmann C, Horak C, Horton L, Klose F, Larese J, Mesecar A, Myles D, Neuefeind J, Ohl M, Tulk C, Wang X L and Zhao J 2006 *Physica B* **385-86** 955–960

[10] Farago B 2009 *Curr. Opin. Coll. Interf. Sci.* **14** 391–395
[11] Pappas C, Kali G, Krist T, Böni P and Mezei F 2000 *Physica B* **283** 365–371
[12] Ollivier J, Mutka H and Didier L 2010 *Neutron News* **21** 22–25
[13] Itoh S, Yokoo T, Satoh S, Yano S i, Kawana D, Suzuki J and Sato T J 2011 *Nucl. Instrum. Meth. Phys. Res. A* **631** 90–97
[14] Fouquet P, Jardine A, Dworski S, Alexandrowicz G, Allison W and Ellis J 2005 *Rev. Sci. Instrum.* **76** 053109
[15] Herwig K, Wu Z, Dai P, Taub H and Hansen F 1997 *J. Chem. Phys.* **107** 5186–5196
[16] Fuhrmann D, Criswell L, Mo H, Volkmann U, Herwig K, Taub H and Hansen F 2000 *Physica B* **276** 345–346
[17] Hansen F, Criswell L, Fuhrmann D, Herwig K, Diama A, Dimeo R, Neumann D, Volkmann U and Taub H 2004 *Phys. Rev. Lett.* **92** 046103
[18] Enevoldsen A D, Hansen F Y, Diama A, Taub H, Dimeo R M, Neumann D A and Copley J R D 2007 *J. Chem. Phys.* **126** 104704
[19] Larese J Z, Arnold T, Barbour A and Frazier L R 2009 *Langmuir* **25** 4078–4083
[20] Wang S K, Mamontov E, Bai M, Hansen F Y, Taub H, Copley J R D, Sakai V G, Gasparovic G, Jenkins T, Tyagi M, Herwig K W, Neumann D A, Montfrooij W and Volkmann U G 2010 *EPL* **91** 66007
[21] Olsen R J, Firlej L, Kuchta B, Taub H, Pfeifer P and Wexler C 2011 *Carbon* **49** 1663–1671
[22] Jardine A P, Dworski S, Fouquet P, Alexandrowicz G, Riley D J, Lee G Y H, Ellis J and Allison W 2004 *Science* **304** 1790–1793
[23] Hedgeland H, Fouquet P, Jardine A P, Alexandrowicz G, Allison W and Ellis J 2009 *Nature Phys.* **5** 561–564
[24] Springer T 1972 *Quasi-elastic neutron scattering for the Investigation of Diffusive Motions in Solids and Liquids* (*Springer Tracts in Modern Physics* vol 64) ed Höhler G (Berlin: Springer)
[25] Lovesey S W 1984 *Theory of Neutron Scattering from Condensed Matter. Volume 1: Nuclear Scattering* (Oxford: Clarendon Press)
[26] Bée M 1988 *Quasielastic Neutron Scattering* (Bristol: Adam Hilger)
[27] Bordallo H N, Aldridge L P, Churchman G J, Gates W P, Telling M T F, Kiefer K, Fouquet P, Seydel T and Kimber S J 2008 *J. Phys. Chem. C* **112** 13982–13991
[28] Fouquet P, Johnson M R, Hedgeland H, Jardine A P, Ellis J and Allison W 2009 *Carbon* **47** 2627–2639
[29] Ala-Nissila T, Ferrando R and Ying S C 2002 *Adv. Phys.* **51** 949–1078
[30] Matties M A and Hentschke R 1996 *Langmuir* **12** 2501–2504
[31] Vernov A and Steele W A 1991 *Langmuir* **7** 2817–2820
[32] Hempelmann R 2000 *Quasielastic neutron scattering and solid state diffusion* (Oxford: Oxford University Press)
[33] Jardine A P, Ellis J and Allison W 2002 *J. Phys.: Condens. Matter* **14** 6173–6191
[34] van Hove L 1954 *Phys. Rev.* **95** 253–262
[35] Furrer A, Mesot J and Strässle T 2009 *Neutron Scattering in Condensed Matter Physics* (*Series on Neutron Techniques and Applications* vol 4) (Singapore: World Scientific)
[36] Barreiro A, Rurali R, Hernández E R, Moser J, Pichler T, Forró L and Bachtold A 2008 *Science* **320** 775–778
[37] Wirtz L and Rubio A 2004 *Sol. State Comm.* **131** 141–152
[38] Calvo-Almazán I and Fouquet P unpublished data
[39] Favro L D 1965 *Fluctuation phenomena in solids* (*Pure and applied physics* vol 19) ed Burgess R E (New York: Academic Press)
[40] Chudley C T and Elliott R J 1960 *Proc. Phys. Soc. Lond.* **LXXVII** 353–361
[41] Barnes J D 1973 *The Journal of Chemical Physics* **58** 5193–5201
[42] Sears V F 1967 *Can. J. Phys.* **45** 237 – 253
[43] Sears V F 1966 *Can. J. Phys.* **44** 1299 – 1311

[44] Martínez-Casado R, Sanz A S, Vega J L, Rojas-Lorenzo G and Miret-Artés S 2010 *Chem. Phys.* **370** 180–193
[45] Martínez-Casado R, Sanz A S, Rojas-Lorenzo G and Miret-Artés S 2010 *J. Chem. Phys.* **132** 054704
[46] Calvo-Almazán I, Seydel T and Fouquet P 2010 *J. Phys.: Condens. Matter* **22** 304014
[47] Spiegel M R, Liu J and Abellanas L 2005 *Mathematical Handbook of Formulas and Tables* 2nd ed (New York: McGraw-Hill)
[48] Gilbert E P, Reynolds P A and White J W 1998 *J. Chem. Soc. - Faraday Trans.* **94** 1861–1868
[49] Guerra R, Tartaglino U, Vanossi A and Tosatti E 2010 *Nature Mat.* **9** 634 – 637
[50] Heidemann A, Magerl A, Prager M, Richter D and Springer T (eds) 1986 *ILL - IFF Workshop* vol 17 (Berlin: Springer-Verlag)
[51] Schiebel P, Prandl W, Wulf K, Papoular R, Paulus W and G H 1997 *Physica B* **234** 64 –65